Available online at www.sciencedirect.com

SciVerse ScienceDirect

Journal of the European Ceramic Society 32 (2012) 1883–1892

www.elsevier.com/locate/jeurceramsoc

Conversion behaviour and resulting mechanical properties of polysilazane-based coatings

Martin Günthner[a], Kaishi Wang[b], Rajendra K. Bordia[b], Günter Motz[a,*]

[a] University of Bayreuth, Ceramic Materials Engineering (CME), D-95440 Bayreuth, Germany

[b] University of Washington, Department of Materials Science and Engineering, Seattle, WA 98195-2120, USA

Abstract

Polymer-derived ceramics exhibit a convenient route for the processing of low-dimensional ceramics like coatings or fibres. In previous investigations unfilled and composite coatings have been developed using ammonolysed bis(dichloromethylsilyl)ethane (ABSE) or perhydropolysilazane (PHPS) as precursors and BN, ZrO_2 or glass particles as filler materials. The coating systems provide excellent corrosion and oxidation resistance to underlying metals. This paper reports on the effect of the precursor system and the pyrolysis parameters on the conversion behaviour, shrinkage and mechanical properties, including hardness and Young's modulus, of ABSE- and PHPS-based coatings. Therefore the crosslinking and pyrolysis behaviour as well as the mechanical properties of the coatings were investigated up to pyrolysis temperatures of 1000 °C in nitrogen and in air by ATR-IR, SEM, profilometry and nanoindentation measurements. The coatings pyrolysed at 1000 °C in nitrogen, have hardness values of 13 GPa and Young's moduli up to 155 GPa.

Keywords: Polymer derived ceramics; A. Films; B. Surfaces; C. Mechanical properties; E. Structural applications

1. Introduction

Silicon-based ceramics like silicon nitride (Si_3N_4) or silicon oxycarbonitride (SiCNO) are promising materials for high temperature and tribological applications in harsh environments because of their very good thermal shock resistance, creep resistance, thermal stability, high temperature strength, corrosion and oxidation stability as well as hardness.[1,2] Si(C)NO films can be deposited by various methods including physical (PVD) and chemical (CVD) vapour deposition techniques.[3,4]

An alternative approach to these vapour phase methods is the processing of Si(C)NO coatings by thermal decomposition of polymer precursors, so called polymer derived ceramics (PDCs). Mainly, precursors like polycarbosilanes, polysilazanes or polysiloxanes are used.[5–8] An overview of this topic has been presented by Scheffler and Torrey.[9] Due to the increasing availability of advanced precursor materials and the easy and low cost coating techniques, several coating systems for low and medium temperature applications in the fields of energy, environment and transportation have been explored.[10,11] Several reports have focused on development, microstructure and performance of PDC coatings as environmental barrier.[12–17] The processing of coatings based on PDCs can be divided into three steps: (i) Synthesis of polymer precursors, (ii) shaping (varnish techniques like spraying or dip coating) followed by crosslinking of the precursors to an infusible network and (iii) conversion into an amorphous or crystalline ceramic by pyrolysis.[10] Thus a good knowledge of the conversion behaviour of the precursors into polymeric- and ceramic-like coatings is essential.

The microstructure, composition and mechanical or chemical properties of PDCs mainly depend on the precursor system, the degree of crosslinking, the pyrolysis temperature and the pyrolysis atmosphere.[8] Concerning the conversion behaviour of PDCs, several publications have focused on the pyrolysis and crystallization behaviour of poly(carbo)silazanes into the corresponding ceramics especially at high temperatures and in inert atmospheres.[5–8,18–23] Other authors describe the curing of polysilazane-based films at room temperature by moisture.[24,25] However, studies on the conversion behaviour and the resulting mechanical properties of precursors and precursor based coatings in the low and medium temperature range up to 1000 °C and the effect of the pyrolysis in air are limited. This paper reports

---

* Corresponding author. Tel.: +49 921 555505; fax: +49 921 555502.
E-mail addresses: martin.guenthner@uni-bayreuth.de (M. Günthner), kshwang@u.washington.edu (K. Wang), bordia@u.washington.edu (R.K. Bordia), guenter.motz@uni-bayreuth.de (G. Motz).

0955-2219/$ – see front matter © 2011 Elsevier Ltd. All rights reserved.
doi:10.1016/j.jeurceramsoc.2011.09.005

on the effect of the precursor system and the pyrolysis parameters on the conversion behaviour, shrinkage and mechanical properties of polysilazane-based coatings.

Ammonolysed bis(dichloromethylsilyl)ethane (ABSE) and perhydropolysilazane (PHPS) were selected as the base materials for the coatings, since in previous studies these systems have been shown to provide excellent oxidation and corrosion protection to steel and nickel-based superalloys.[14–17] Furthermore they have fundamentally different chemical structures: The ABSE system is an organic polycarbosilazane with an excess of carbon, whereas the inorganic polysilazane PHPS exhibits an excess of silicon. Thus the use of two different precursor materials enables the investigation of the effect of precursor chemistry on the conversion behaviour as well as the mechanical properties. After dissolving the polymers in organic solvents like toluene or ether, different metallic and glass substrates were dip coated with suitable precursor solutions. In order to examine the effect of the pyrolysis atmosphere and temperature, the crosslinking and thermal treatment were performed in air or in nitrogen up to 1000 °C, which led to the formation of Si(C)NO-coatings. The conversion behaviour as well as the mechanical properties of the polysilazane-based coatings has been studied by attenuated total reflectance infrared spectroscopy (ATR-IR), scanning electron microscopy (SEM), energy dispersive X-ray spectroscopy (EDS), profilometry and nanoindentation experiments.

2. Experimental procedure

As already described, the ABSE polycarbosilazane is synthesised by ammonolysis of bis(dichloromethylsilyl)ethane in toluene.[26] For the processing of coatings, the resulting colourless, brittle and meltable solid precursor can be dissolved in toluene or ether.

The commercially available PHPS polysilazane is produced by ammonolysis of dichlorosilane SiH_2Cl_2.[27] A solution of 20% by weight in dibutylether was used (PHPS NN 120-20, Clariant Advanced Materials GmbH, Germany).

Flat plates of stainless steel (AISI 304, AISI 430), glass and fused silica were cleaned in acetone by ultrasonic treatment and dried. The samples were dip-coated with a hoisting apparatus and the coating thickness was adjusted by concentration of the solution and by variation of the hoisting speed between 1.5 and 8 mm/s. The annealing of the coated samples was performed in air (Nabertherm® LH 60/14, Nabertherm, Germany) or in nitrogen (F-A 100-500/13, GERO GmbH, Germany) at temperatures up to 1000 °C with heating and cooling rates of 3 K/min.

The conversion of the coatings was examined by ATR-FTIR spectroscopy (Avatar 370 FT-IR spectrometer, Thermo Nicolet Corporation, USA) and scanning electron microscopy with EDX (1540EsB Cross Beam, Carl Zeiss AG, Germany).

The layer thickness was measured with a Fischerscope® MMS (Helmut Fischer GmbH & Co. KG, Germany) corresponding to the eddy current method (ASTM B244) or by the profile method (DIN EN ISO 4287/MFW-250 Mahr GmbH, Germany). The most accurate and reproducible results could be achieved by profilometry. In this technique, a tip moves horizontally over the surface and the vertical displacement is measured. In order to investigate the coating thickness, the polymeric coatings were scratched with a sharp cutter and afterwards the surface profile was detected by the tip. The coating thickness d was measured both before (d_0) and after the respective thermal treatment (d_1) on coated glass or fused silica samples. Hence the coating shrinkage can be calculated as:

$$\text{Shrinkage}_{\text{coating}} = \left| \frac{d_1 - d_0}{d_0} \right| \tag{1}$$

Additionally the volume shrinkage of the coatings was calculated by the mass and density values in the initial state (m_0, ρ_0) and after the respective thermal treatment (m_1, ρ_1) according to Eq. (2):

$$\text{Volume shrinkage}_{\text{calculated}} = \left| \frac{V_1 - V_0}{V_0} \right| = \left| \frac{(m_1/\rho_1) - (m_0/\rho_0)}{(m_0/\rho_0)} \right| \tag{2}$$

Nanoindentation was performed to determine the film hardness and Young's modulus using a Nano Indenter® G200 (MTS Nano Instruments) with a Berkovich diamond indenter. 15 indents were applied on each sample with an indentation depth up to 1 μm. The data was averaged for an indentation depth of 100 nm (approximately 10% of the film thickness). The resulting load displacement curves were evaluated according to the Oliver and Pharr model.[28] From the data the hardness H can be calculated using the equation:

$$H = \frac{P_{\max}}{A} \tag{3}$$

where A is the area of the indentation at a maximum applied load $P_{\max}$.

Furthermore the reduced modulus (E_r) is calculated from the slope of the unloading curve according to the following equation:

$$E_r = S * \frac{\sqrt{\pi}}{2\sqrt{A}} \tag{4}$$

where S is the unloading stiffness and A the projected contact area.

The Young's modulus E_1 of the tested material 1 for a given Poisson's ratio ν_1 is calculated as:

$$\frac{1}{E_r} = \frac{(1-\nu_1^2)}{E_1} + \frac{(1-\nu_2^2)}{E_2} \tag{5}$$

where E_2 and ν_2 are the modulus and the ratio of the indenter tip ($E_2 = 1140$ GPa and $\nu_2 = 0.07$).

In order to investigate the conversion behaviour of the polysilazanes, fine precursor powders were used. For a better comparability with the behaviour of the coatings the precursor powders were milled and sieved to a grain size smaller than 32 μm. The powders were cured in nitrogen or in air at temperatures up to 1000 °C according to the thermal treatment of the coatings. Different powder fractions were analysed by thermogravimetry (TGA) (Linseis L81 A1550, Linseis, Germany), coupled both with infrared spectroscopy (Bruker Vector 22,

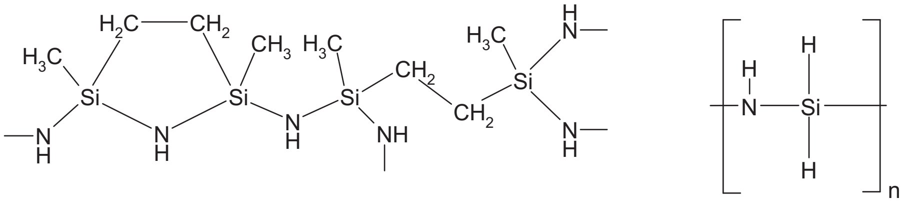

Fig. 1. Basic structure units of the ABSE (left) and PHPS (right) precursor.

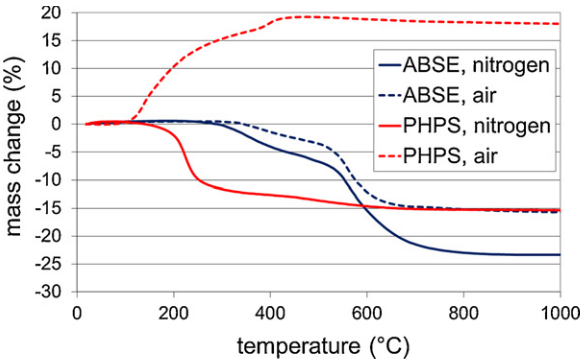

Fig. 2. TG analyses of ABSE and PHPS powders (<32 μm) in nitrogen and air.

Bruker Optik GmbH, Germany) and mass spectrometry units (ThermoStar GSD 301 T3, Pfeiffer Vacuum GmbH, Germany). The chemical composition was investigated by "Mikroanalytisches Labor Pascher" in Germany.

3. Results and discussion

3.1. Conversion behaviour of ABSE and PHPS polysilazanes

The chemical structure of the polycarbosilazane ABSE consists of two structural elements namely stable 5-membered carbosilazane rings and bridging linear carbosilazane units (Fig. 1).[26] Depending on the molecular weight the melting point varies from 90 up to 150 °C.

In contrast to the ABSE precursor, the commercially available PHPS precursor contains no organic groups (see Fig. 1). Due to the large number of Si–H bonds, the PHPS is highly reactive with hydroxyl groups.[14,24]

Milled powders of the two different polysilazanes were already used to investigate the pyrolysis behaviour.[14] The results (see also Fig. 2) can be summarized as follows.

The mass change mainly depends on the precursor system, the pyrolysis temperature and the pyrolysis atmosphere. After the crosslinking of the polymers at temperatures up to 200 °C for PHPS and 300 °C for ABSE respectively, the conversion of the polysilazanes into the corresponding ceramics starts, which is characterised by an explicit mass change. Due to the inorganic nature of the PHPS system, the conversion of PHPS occurs at lower temperatures and is associated with a higher ceramic yield. After pyrolysis temperatures of 700 °C for PHPS and 800 °C for ABSE, the mass change is completed. The pyrolysis in air leads in both cases to an increase of the ceramic yield due to the incorporation of oxygen.

In order to get a better understanding of the conversion behaviour of the coatings, ATR-IR analyses were performed on the ABSE- and PHPS-based coatings. The correlation of the signals in the IR-absorption spectra to the respective functional groups was carried out according to available data from literature, which are summarized in Table 1.

The characteristic ATR-IR spectra of the polysilazane-based coatings on the steel AISI 304 as a function of the pyrolysis temperature and the pyrolysis atmosphere are displayed in Fig. 3.

It can be seen for all coatings that the intensity of the absorption bands and therefore the number of functional groups decrease with increasing pyrolysis temperature. This is typical for the conversion of the polymers into ceramic-like systems.

The spectra of the ABSE-based coatings after pyrolysis in nitrogen (see Fig. 3a) show, that after curing temperatures of 150 and 300 °C the characteristic bands for the N–H, C–H and Si–CH_3 groups are present. The crosslinking of the thin coatings by transamination[30] (see Eq. (6)) is not yet fully completed at 300 °C.

$$3{\equiv}\text{Si–NH–Si}{\equiv} \rightarrow 2\text{N}(\text{Si}{\equiv})_3 + \text{NH}_3 \qquad (6)$$

After 500 °C, the signals for the N–H groups disappear, while the bands of the C–H and Si–CH_3 groups are still detectable. This correlates very well with results from FTIR-coupled TGA-measurements,[14] which identified mainly the separation of

Table 1
Characteristic IR-absorption bands of different functional groups.[23,24,29]

Wavenumber (cm^{-1})	Vibration band, vibration mode	Wavenumber (cm^{-1})	Vibration band vibration mode
3400, 3380	N–H, valence	1170, 1167	N–H, deformation
2963, 2950	C(sp^3)–H, valence	1200–1000	Si–O–Si, valence
2905, 2870	C(sp^3)–H, valence	1020–820	Si–N–Si, Si–C–Si
2160, 2090	Si–H, deformation	989	Si–CH_2–CH_2–Si
1390–1370	–CH_3, deformation	912	Si–H, deformation
1266, 1250	Si–CH_3, deformation	800–790	Si–O–Si, valence

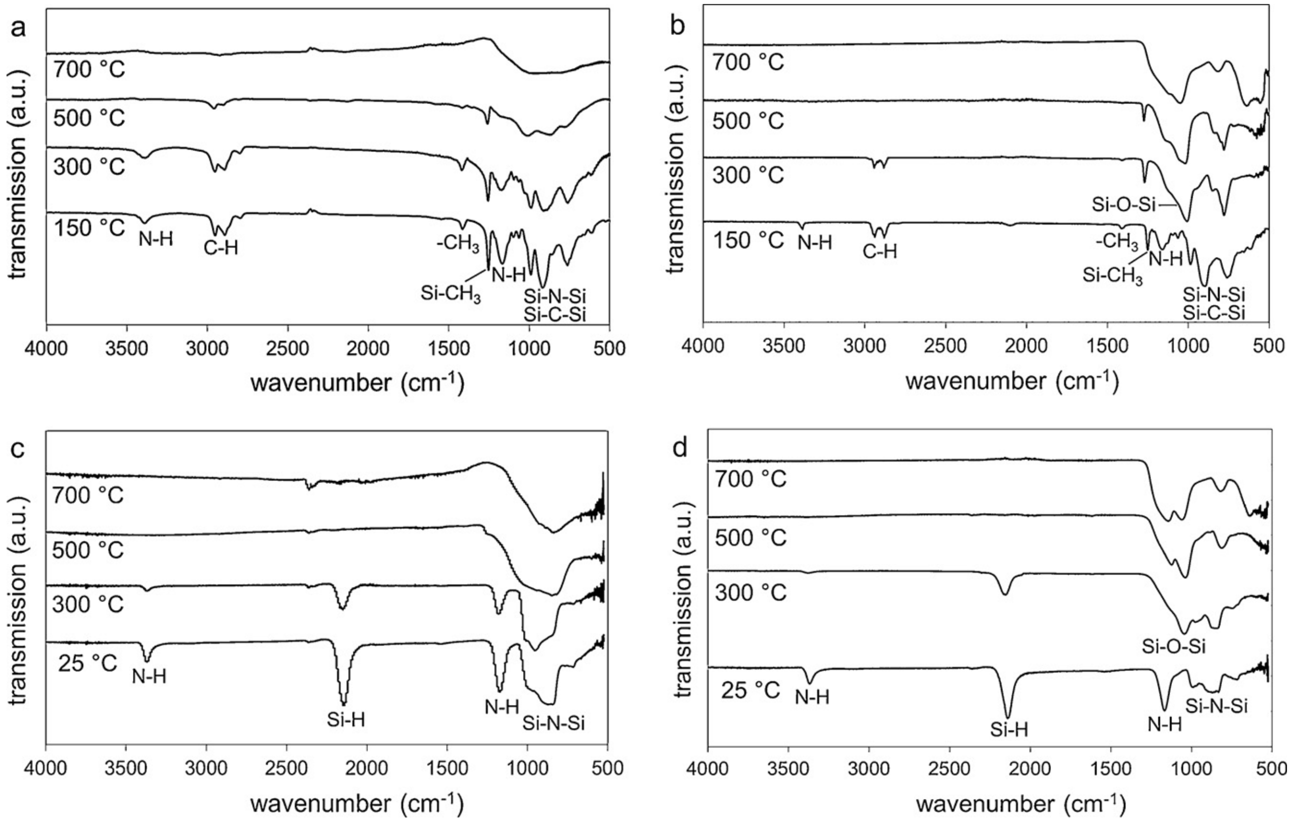

Fig. 3. ATR-IR transmission spectra of polysilazane-based coatings on steel AISI 304 as a function of pyrolysis temperature and pyrolysis atmosphere (thermal treatment with 1 h holding time, 3 K/min heating and cooling rate): (a) ABSE, nitrogen; (b) ABSE, air; (c) PHPS, nitrogen; (d) PHPS, air.

ammonia between 300 and 500 °C. After a pyrolysis temperature of 700 °C also the characteristic absorption bands of the C–H and $Si–CH_3$ groups disappear due to the release of methane. In the fingerprint region (<1500 cm^{-1}) a broad band between 1100 and 800 cm^{-1} occurs which is typical for an amorphous SiCN-system. The broadening of the signal to higher wavenumbers indicates the existence of Si–O–Si groups resulting from oxygen impurities. The incorporation of oxygen was also detected by GDOES and chemical composition measurements of ABSE-derived coatings and powders pyrolysed in nitrogen.[14]

The characteristic absorption bands of the ABSE-derived coatings after pyrolysis in air are displayed in Fig. 3b. Analogous to the thermal treatment in nitrogen, the signals of the N–H, C–H and $Si–CH_3$ groups are present after curing at 150 °C. After a thermal treatment at 300 °C the absorption band of the N–H group disappears. Additionally the bands for the Si–O–Si groups with wavenumbers between 1200 and 1000 cm^{-1} and in the range of 800 cm^{-1} can be identified. Thus the substitution of the N–H groups by the reaction of ABSE with moisture and consequently the formation of Si–O–Si bonds according to Eq. (7) is the main crosslinking reaction.[31]

$$\equiv Si_2–NH + H_2O \rightarrow (\equiv Si–OH + \equiv Si–NH_2)$$
$$\rightarrow \equiv Si–O–Si\equiv + NH_3 \tag{7}$$

The crosslinking of the ABSE polysilazane in air consequently takes place at lower temperatures compared to the curing in nitrogen. This fact was also found in a recent publication by Chavez et al.[32] They investigated the effect of ambient atmosphere on the crosslinking of polysilazanes. Up to a temperature of 500 °C, C-containing (especially $Si–CH_3$) groups are detectable. Above 700 °C all characteristic bands of hydrogen containing functional groups disappear. Only the absorption bands of the Si–O–Si-groups between 1200 and 1000 cm^{-1} and in the range of 800 cm^{-1} are present. These findings correlate very well with results of GDOES-depth profile and chemical composition measurements on ABSE-derived coatings or fine powders. After pyrolysis in air at temperatures >700 °C, the composition of the coatings and powders was mainly SiO_2.[14]

The absorption spectra of the PHPS coatings at room temperature in nitrogen (Fig. 3c) show the characteristic bands of the N–H (3380 and 1170 cm^{-1}) as well as the Si–H bonds (2160 cm^{-1}). After curing at 300 °C the intensity of the signals decrease indicating that the crosslinking of the polymer by the dehydrocoupling reaction[33] (see Eq. (8)) is not finished yet.

$$\equiv Si–H + {=}N–H \rightarrow \equiv Si–N{=} + H_2 \tag{8}$$

After pyrolysis temperatures >500 °C the signals of the N–H and Si–H groups disappear. A broad absorption band between 1100 and 820 cm^{-1} exhibits the presence of a silicon nitride ceramic. The slight shift to higher wavenumbers, which was also observed for the ABSE coatings (see Fig. 3a), again indicates an incorporation of oxygen and the formation of Si–O–Si bonds.

Fig. 3d displays the ATR-IR spectra of the PHPS-based coatings after heating in air up to 700 °C. After a treatment at room temperature for 1 h in air the signals for the N–H, Si–H and Si–N–Si groups were detected. After 300 °C the signals decrease but are still present. Additionally an absorption band for the Si–O–Si groups between 1100 and 1000 cm^{-1} is observed. No signals of hydrogen containing groups can be observed after pyrolysis at 500 °C or 700 °C. In the fingerprint region two absorption bands between 1200 and 1000 cm^{-1} as well as between 870 and 800 cm^{-1} indicate the presence of both Si–O–Si and Si–N–Si groups. Bauer et al.[24] published similar results for the curing behaviour of PHPS-based coatings in moisture. They demonstrated that the PHPS-derived coatings can be crosslinked by moisture leading to a conversion of the polysilazane-based films into SiO_x-coatings at relatively low temperatures (used parameters[24]: moisture, 150 °C, PHPS system with basic catalyst). Our results of the ATR-IR, GDOES and chemical composition measurements[14] show, that under the chosen conditions (air, no catalyst) full transformation of the PHPS-based coatings into SiO_x does not take place.

In summary, ATR-IR measurements are a useful tool to investigate the main crosslinking and pyrolysis reactions of the polysilazane-based coatings. After thermal treatment in air the characteristic bands of the Si–O–Si groups occur at temperatures higher than 300 °C. Furthermore the conversion of the polymers is shifted to lower temperatures by a thermal treatment in air. The findings are in good agreement to the results of the TGA, GDOES and chemical composition measurements on ABSE- and PHPS-based powders and coatings.[14]

3.2. Shrinkage of polysilazane-based coatings

The conversion of the polymers into ceramic systems is associated with a mass change and an explicit density increase. The resulting shrinkage leads to a reduction of the coating thickness and is the main drawback of the precursor technology. The shrinkage limits the coating thickness since thicker coatings result in cracking due to constrained pyrolysis.

As already mentioned the volume shrinkage of the polysilazanes ABSE and PHPS was calculated by the density values[18,34,35] and weight change (see Section 3.1) of the systems according to Eq. (2). Fig. 4 shows the calculated volume shrinkage of both precursors as a function of the pyrolysis temperature and the pyrolysis atmosphere.

The crosslinking of the polymers up to 200 °C (PHPS) and 300 °C (ABSE) respectively is associated with a volume shrinkage of about 15%. In the temperature range between 200 and 700 °C (PHPS) or 300 and 800 °C (ABSE) the most significant volume change occurs due to the typical pyrolysis effects like weight loss and density increase. Fig. 4 also shows that – compared to the ABSE system – the conversion of the PHPS polysilazane into a ceramic material is completed at lower temperatures. While no further mass loss is detected at temperatures higher than 800 °C (see Fig. 2) the volume continues to decrease above 800 °C. This is due to structural rearrangement processes, which result in a further compaction (densification) of the ceramics. After a thermal treatment in nitrogen at 1000 °C the volume shrinkage of the systems is higher than 60%.

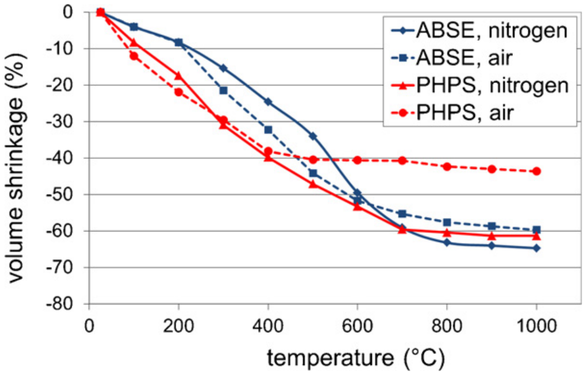

Fig. 4. Volume shrinkage of the polymers ABSE and PHPS as function of the pyrolysis temperature and the pyrolysis atmosphere (calculated according to Eq. (2)).

The thermal treatment in air leads to a reduced shrinkage for both precursors. The reason for that is the incorporation of oxygen leading to a higher ceramic yield. However, the shrinkage of the PHPS polymer is lower than ABSE. This is due to the partially free Si-content in the PHPS system formed during pyrolysis. Oxidation to mainly SiO_x leads to a significant mass gain during thermal treatment in air (see Fig. 2) and also to a reduced shrinkage. In contrast, the free C-content of the ABSE polysilazane is partially oxidised to gaseous CO_2. Thus the volume shrinkage of the PHPS system in air is about 15% lower than that of the ABSE polymer.

The shrinkage of the polysilazane-based coatings was experimentally determined by measuring the coating thickness before and after the thermal treatment according to Eq. (1). The decrease in coating thickness thereby corresponds to volume shrinkage, since shrinkage in the coating plane is not possible due to the bonding of the coatings on the substrates. In order to exclude incorrect results caused by coating failures, the investigations were performed on pore and crack free thin coatings with a thickness of about 1 μm, which was verified by scanning electron microscopy. Typical ABSE- and PHPS-based coatings after different pyrolysis conditions are shown in Fig. 5.

In Fig. 6, the experimentally determined shrinkage of the coatings is displayed. For clarity reasons, the standard deviation with values up to 20%, which results from measuring errors and deviations in the coating thicknesses, is not plotted.

The experimentally determined shrinkage of the coatings agrees very well with the calculated shrinkage behaviour shown in Fig. 4. Once again the faster conversion of the PHPS-based coatings can be detected. Furthermore, a treatment in air results in lower shrinkage compared to a pyrolysis in nitrogen.

Motz and Ziegler[35] as well as Colombo et al.[36] also investigated the shrinkage behaviour of Ti- and Zr-modified polysilazane-based or polycarbosilane-based coatings. They published similar shrinkage characteristics and slightly different shrinkage values (up to 40%[35] or up to 80%[36]). The likely reasons for these differences are different precursors and different methods for measuring the coating thickness.

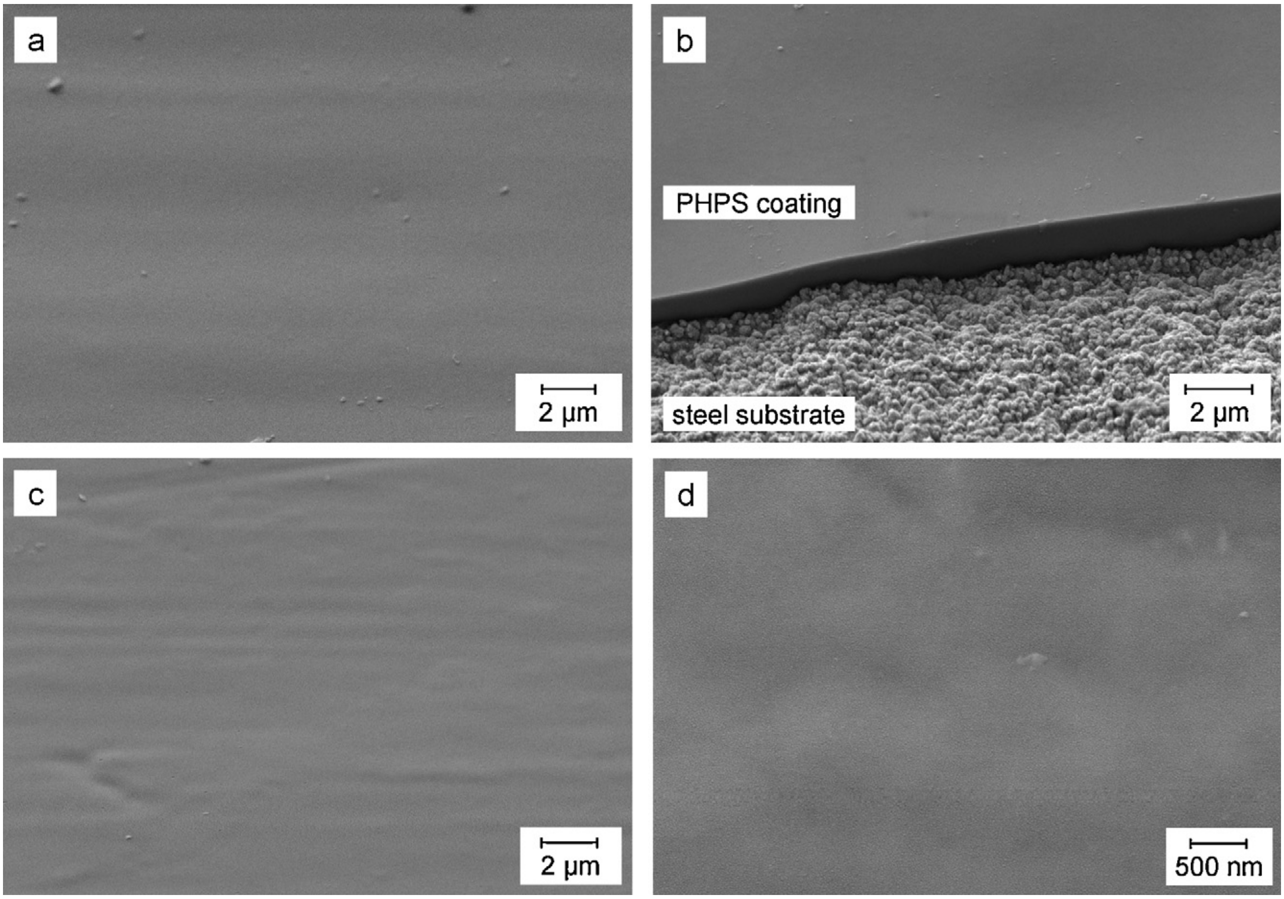

Fig. 5. Scanning electron micrographs of different polysilazane-based coatings on steel AISI 304 (1 h, 3 K/min): (a) PHPS, 200 °C, air; (b) PHPS, 300 °C, air; (c) PHPS, 500 °C, nitrogen; (d) ABSE, 800 °C, air.

It can further be seen from Fig. 6, that the shrinkage of the coatings between 800 °C and 1000 °C in nitrogen is rather high This indicates that a sublimation of gaseous products, especially SiO takes place above 900 °C, which was also found by other authors.[31,37] Oxygen is incorporated into the thin PDC coatings resulting from impurities or from oxygen contaminations in the pyrolysis atmosphere (see Section 3.1). The low oxygen partial pressure in the pyrolysis atmosphere ($O_2 < 50$ vpm) therefore cannot lead to a complete oxidation to SiO_2. Thus the formed SiO, which has a high vapour pressure at $T > 900$ °C, partially sublimates leading to an additional weight loss and shrinkage of the coatings.

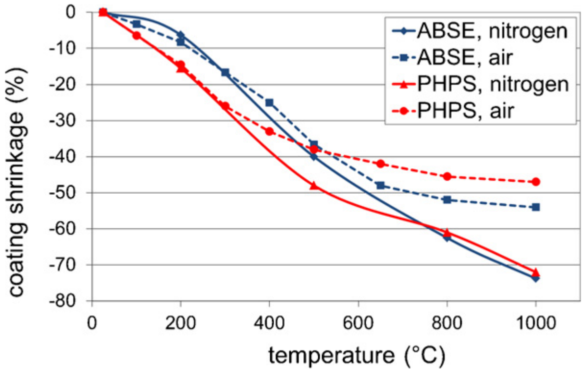

Fig. 6. Experimental shrinkage of the ABSE- and PHPS-based coatings as function of the pyrolysis temperature and the pyrolysis atmosphere (according to Eq. (1)).

The critical coating thickness, up to which dense and crack-free coatings can be applied, mainly depends on the shrinkage values. Because of the less shrinkage of the PHPS system the critical coating thickness of the PHPS-based coatings should be higher than that of the ABSE-derived films. This could be proved by scanning electron microscopy. Fig. 7 shows an ABSE- and a PHPS-based coating with a thickness of about 1 μm after pyrolysis in air at 800 °C. Whereas the ABSE-based coating exhibits several shrinkage cracks, no cracks are visible for the PHPS-based coatings.

Altogether, the shrinkage behaviour correlates well with the conversion behaviour discussed in Section 3.1. The calculated volume shrinkage values are very similar to the experimentally determined shrinkage values for both coatings in the two atmospheres. After pyrolysis at 1000 °C the shrinkage values vary between 45% and 75%. The PHPS-based coatings exhibit lower shrinkage compared to the ABSE-derived coatings leading to a higher critical coating thickness before constrained pyrolysis induced cracks are observed.

3.3. Mechanical properties of polysilazane-based coatings

Using nanoindentation the hardness and Young's modulus of about 1 μm thick ABSE- and PHPS-based coatings on steel AISI

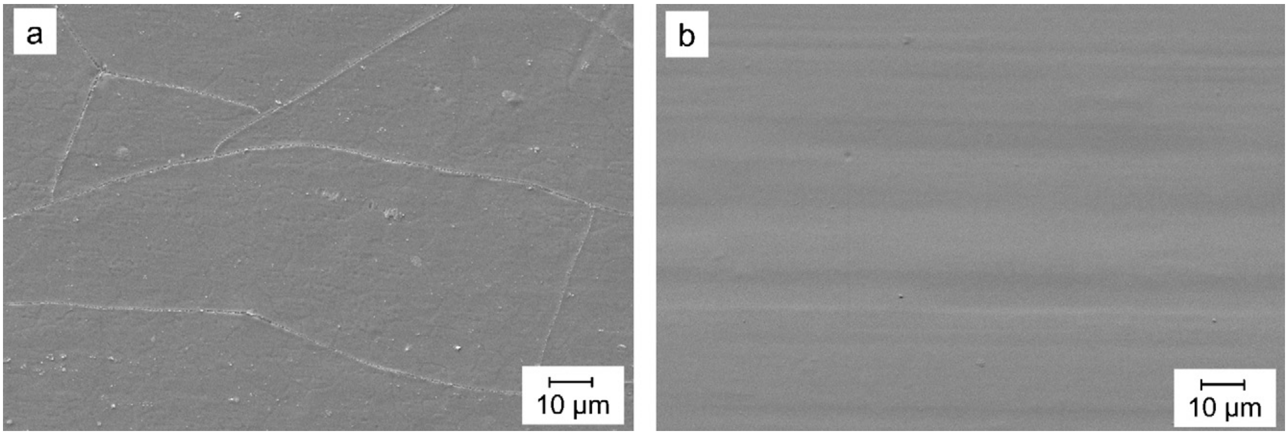

Fig. 7. Scanning electron micrographs of about 1 μm thick ABSE-derived (a) and PHPS-based (b) coatings on steel AISI 304 after a pyrolysis at 800 °C in air (1 h, 3 K/min).

430 were investigated. 15 indents were conducted at room temperature on each sample with an indentation depth up to 1 μm. For plotting the coating hardness as a function of the pyrolysis temperature and the pyrolysis atmosphere (see Fig. 8), the data are averaged for an indentation depth of 100 nm (approximately 10% of the film thickness).

It can be seen from the diagram that the hardness of the coatings increases with the pyrolysis temperature. For the ABSE precursor, the hardness of the crosslinked coatings after a curing temperature up to 500 °C is only 1 GPa (curing in nitrogen) or 2 GPa (curing in air). Because of the conversion of the polymer into an amorphous ceramic, the hardness increases to a value of about 12 GPa after a pyrolysis at 1000 °C.

The PHPS system is characterised by higher hardness values in the temperature region up to 700 °C. This is due to its inorganic nature resulting in a rapid crosslinking and a less mass change during pyrolysis. Thus a hardness of about 6 GPa is already reached after a thermal treatment at 500 °C in nitrogen. At higher temperatures (>800 °C), the hardness of the PHPS-based coatings is similar to that for the ABSE-derived films, since at these temperatures, the conversion of both precursors into the corresponding ceramic is complete.

Further the pyrolysis atmosphere has a significant influence on the hardness of the coatings. The thermal treatment in air leads to higher hardness values in the temperature region up to 400 °C, since the crosslinking in air is faster than that in nitrogen (see Section 3.1). At temperatures >800 °C, the hardness of the coatings pyrolysed in nitrogen is higher than the hardness of the coatings treated in air. This is due to the incorporation of oxygen during pyrolysis in air. The resulting coatings with a chemical composition of approximately SiO_2 show a lower hardness than the Si(C)N-coatings. However the ABSE- and PHPS-based coatings pyrolysed in air at 950 °C have slightly higher hardness values than pure SiO_2 (fused silica: 8–10 GPa).[38] This points out that additional hetero-atoms like C or N are present in the coatings.

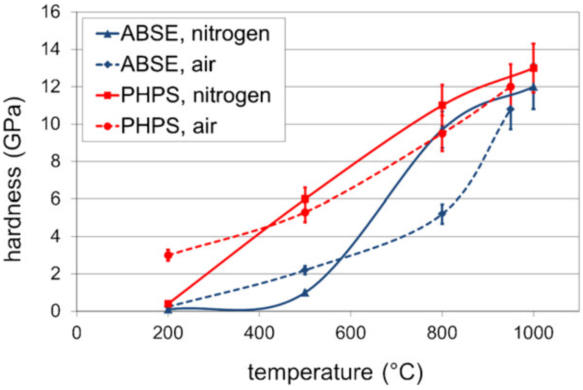

Fig. 8. Hardness of ABSE- and PHPS-based coatings on steel AISI 430 as function of the pyrolysis temperature and the pyrolysis atmosphere (1 h, 3 K/min).

The comparison of our investigated hardness data with values published by other authors[21,34] affirms, that the hardness of precursor systems increases with the pyrolysis temperature. The quantitative hardness values mainly depend on the measuring technique, the indentation load and the geometry or the pre-treatment of the samples. Additionally for PDC ceramics the processing parameters like pyrolysis temperature or atmosphere, inhomogeneities like pores or C-clusters as well as the chemical composition play a major role. In summary, the hardness of the coatings is mainly controlled by the pyrolysis temperature, which however is limited by the respective substrate material. After a pyrolysis at 1000 °C in nitrogen, hardness values up to 13 GPa can be achieved.

The Young's modulus of the coatings was determined using nanoindentation and calculated according to Eqs. (4) and (5). In Fig. 9, the Young's modulus of the ABSE- and PHPS-derived coatings is displayed as a function of the pyrolysis temperature and the pyrolysis atmosphere. The data – analogous to the hardness measurements – represent average values of 15 measurements with an indentation depth of 100 nm on approximately 1 μm thick coatings.

It can be seen from the diagram that the Young's modulus values clearly increase with the pyrolysis temperature. The Young's modulus of the polymeric ABSE-based coating is only 15 GPa after curing at 500 °C. At higher temperatures, the modulus reaches values up to 145 GPa (1000 °C, nitrogen).

The PHPS-based coatings exhibit higher modulus values in the temperature region up to 800 °C than the ABSE-derived

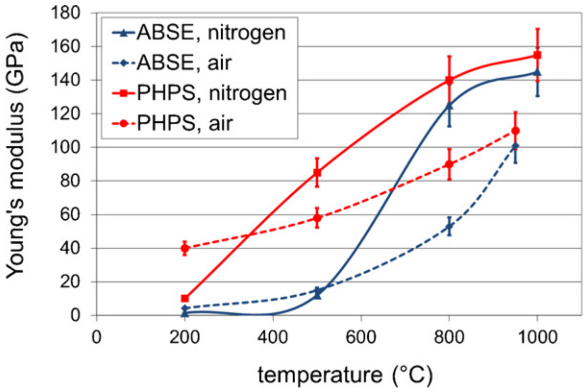

Fig. 9. Young's moduli of ABSE- and PHPS-based coatings on steel AISI 430 as function of the pyrolysis temperature and the pyrolysis atmosphere (1 h, 3 K/min).

films. After pyrolysis temperatures of 950 and 1000 °C, no significant difference between the Young's moduli of the two coating systems can be detected.

Furthermore, an explicit dependence of the Young's modulus on the pyrolysis atmosphere is present. In the polymeric state up to 300 °C for PHPS and up to 500 °C for ABSE higher Young's modulus values can be achieved by a thermal treatment in air. Above these temperatures the values after a pyrolysis in nitrogen are clearly higher. For instance the Young's modulus of the ceramic coatings after a pyrolysis at 1000 °C in nitrogen exhibit values of about 150 GPa, whereas only 110 GPa are achieved after a pyrolysis at 950 °C in air. This can be explained by the higher Young's modulus values of non-oxide ceramics (SiC, Si_3N_4) compared to oxidic systems such as SiO_2 (see also Table 2). While oxide ceramics exhibit mainly ionic bonds, covalent bonds predominate for non-oxide ceramics, which are characterised by a higher bonding strength.[2] However, the reduced Young's moduli of the coatings pyrolysed in air lead to an increased compliance of the coatings at mechanical loads.[1] The higher compliance results in a more strain tolerant behaviour under cyclic thermal loading.

Table 2
Hardness and Young's moduli of different materials.

Material	Hardness (GPa)	Young's modulus (GPa)	Reference
Steel AISI 430	2.5	210	[a]
Fused silica SiO_2	8.6–9.8	72.5	38
Si_3N_4, sintered, dense	15–18	250–330	2
SiC, sintered, dense	25–26	370–450	2
SiCN, crystalline, 1800 °C	16–18	–	7
SiCNO, amorphous, 1000 °C	12	97	39
SiCN, amorphous, 1000 °C	8	100	34
SiCN, amorphous	13	121	40
SiCN-coating (PVD), amorphous	6–12	74–118	3
SiCN-coating (PVD), amorphous	20	210	41
SiCN-coating (CVD), amorphous	12–19	113–181	4
Si_xN_y-coating, amorphous, 1100 °C	4	71	42
SiN(CO)-coating, 1000 °C, N_2	12–13	145–155	[a]
SiO(CN)-coating, 950 °C, air	10–12	100–110	[a]

[a] Internal measurements.

The Young's modulus values between 100 and 110 GPa after a pyrolysis in air at 950 °C further prove that the coatings do not completely convert into SiO_2 systems. Compared to fused silica the values are about 30 GPa higher, which is a confirmation for the existence of additional atoms like C or N in the coatings. This phenomenon was also postulated for the hardness measurements.

In Table 2 the hardness and Young's moduli of different materials and coatings are shown.

The hardness values of the ABSE- and PHPS-based ceramic coatings are higher than the hardness of the most metals or glasses. However, they are not as high as those obtained for crystalline ceramics or coatings, which are mainly applied by PVD- or CVD-techniques. Thus, the thin precursor derived amorphous coatings are not very suitable for heavily loaded mechanical applications. However, a significant hardness increase can be achieved by these coatings on relatively soft substrate materials like stainless steel. Therefore applications of the films as scratch-resistant coatings on soft metals are a possibility.

The determined Young's modulus values of the PDC coatings are – especially after a pyrolysis in nitrogen – relatively high. A comparison with published data (see Table 2) illustrates, that the measured values are higher than the Young's modulus values of monolithic amorphous SiCN-ceramics. This maybe due to the more complete conversion of the coatings due to the short diffusion distances or due to lower levels of porosity in the coatings compared to bulk materials.

4. Conclusion

This work focused on the conversion behaviour as well as the hardness and Young's moduli of ABSE- and PHPS-based coatings. Special emphasis was placed on the effect of pyrolysis in air. The results of the spectroscopic and analytic measurements on the coatings show that the conversion behaviour and the mechanical properties depend not only on the precursor system, but also on the pyrolysis temperature and the pyrolysis atmosphere. After crosslinking of the polysilazanes, the transformation of the polymers into amorphous ceramics takes place at temperatures up to 700 °C for PHPS and 800 °C for ABSE. Due to the inorganic nature of the PHPS system, the conversion of PHPS occurs not only at lower temperatures but is also associated with a higher ceramic yield and lower shrinkage values. Furthermore, for applications in the intermediate temperature range, the processing and thermal treatment of the coatings is possible in air. The following important points must be considered for a pyrolysis in air when compared to a thermal treatment in inert atmospheres:

- Processing in air is more cost effective because it does not require atmosphere control equipment.
- The conversion of the polymers into ceramic-like systems takes place at lower temperatures, minimizing the thermal stresses on the substrate materials.
- The ceramic yield can be increased by incorporating oxygen, leading to reduced shrinkage and making it possible to create thicker coatings without cracks or defects.

- The hardness and Young's moduli of the oxygen-rich coatings are lower compared to pyrolysis in an inert atmosphere, resulting in superior compliance of the coatings under mechanical stresses.

After pyrolysis at 1000 °C in nitrogen, the ceramic coatings are characterised by high hardness values of 13 GPa and Young's moduli up to 155 GPa, which is an evidence for the formation of dense and homogeneous coatings without failures. These coatings have already been shown to be excellent corrosion and environmental barrier coatings. The results of this study demonstrate that they also have good mechanical properties.

Acknowledgements

The authors would like to thank the Bavarian State Ministry of Economy, Infrastructure, Transport and Technologies, Germany and the companies Clariant AG and EnBW Kraftwerke AG as a part of the research initiative "KW21" (Project No. BY7DE) for financial support. Special thanks also go to the chair of metals and alloys, to the chair of functional materials (both University of Bayreuth) and to Dr. Holger Pfaff (Surface Nanolab, Germany) for their support in SEM, profilometry and nanoindentation measurements. The work at University of Washington was supported by a grant from the US Air Force Office of Scientific Research under Award Number AFOSR FA9550-09-1-0633.

References

1. Jacobson NS, Opila EJ, Lee KN. Oxidation and corrosion of ceramics and ceramic matrix composites. *Curr Opin Solid State Mater Sci* 2001;**5**:301–9.
2. Kollenberg W. Technische Keramik [Engineering ceramics]. Essen; 2004.
3. Sundaram KB, Alizadeh Z, Todi RM, Desai VH. Investigations on hardness of rf sputter deposited SiCN thin films. *Mater Sci Eng* 2004;**A368**:103–8.
4. Probst D, Hoche H, Zhou Y, Hauser R, Stelzner T, Scheerer H, et al. Development of PE-CVD Si/C/N:H films for tribological and corrosive complex-load conditions. *Surf Coat Technol* 2005;**200**:355–9.
5. Colombo P, Riedel R, Soraru GD, Kleebe HJ. *Polymer derived ceramics: from nano-structure to applications*. Lancaster: DEStech Publications; 2009.
6. Riedel R, Mera G, Hauser R, Klonczynski A. Silicon-based polymer-derived ceramics: synthesis properties and applications – a review. *J Ceram Soc Jpn* 2006;**114**(6):425–44.
7. Kroke E, Li YL, Konetschny C, Lecomte E, Fasel C, Riedel R. Silazane-derived ceramics and related materials. *Mater Sci Eng* 2000;**26**:97–199.
8. Colombo P, Mera G, Riedel R, Soraru GD. Polymer-derived ceramics: 40 years of research and innovation in advanced ceramics. *J Am Ceram Soc* 2010;**97**(7):1805–37.
9. Scheffler F, Torrey JD. Coatings. In: Colombo P, Riedel R, Soraru GD, Kleebe HJ, editors. *Polymer derived ceramics: from nano-structure to applications*. Lancaster: DEStech Publications; 2009. p. 358–68.
10. Greil P. Polymer derived engineering ceramics. *Adv Eng Mater* 2000;**2**:339–48.
11. Lukacs A. Polysilazane precursors to advanced ceramics. *Am Ceram Soc Bull* 2007;**86**:9301–6.
12. Woiton M, Heyder M, Laskowsky A, Stern E, Scheffler M, Brabec CJ. Self-assembly microstructured polymeric and ceramic surfaces. *J Eur Ceram Soc* 2011;**31**:1803–10.
13. Gardelle B, Duquesne S, Vu C, Bourbigot S. Thermal degradation and fire performance of polysilazane-based coatings. *Thermochim Acta* 2011;**519**:28–37.
14. Günthner M, Kraus T, Dierdorf A, Decker D, Krenkel W, Motz G. Advanced coatings on the basis of Si(C)N precursors for protection of steel against oxidation. *J Eur Ceram Soc* 2009;**29**:2061–8.
15. Günthner M, Kraus T, Dierdorf A, Decker D, Krenkel W, Motz G. Particle-filled PHPS silazane-based coatings on steel. *Int J Appl Ceram Technol* 2009;**6**(3):373–80.
16. Günthner M, Schütz A, Glatzel U, Wang K, Bordia RK, Greißl O, et al. High performance environmental barrier coatings. Part I: passive filler loaded SiCN system for steel. *J Eur Ceram Soc* 2011;**31**:3003–10.
17. Wang K, Günthner M, Motz G, Bordia RK. High performance environmental barrier coatings. Part II: active filler loaded SiOC system for superalloys. *J Eur Ceram Soc* 2011;**31**:3011–20.
18. Schwab ST, Graef RC, Blanchard CR, Dec SF, Maciel GG. The pyrolytic conversion of perhydropolysilazane into silicon nitride. *Ceram Int* 1998;**24**:411–4.
19. Iwamoto Y, Völger W, Kroke E, Riedel R. Crystallization behavior of amorphous silicon carbonitride ceramics derived from organometallic precursors. *J Am Ceram Soc* 2001;**84**(10):2170–8.
20. Funayama O, Tashiro Y, Kamo A, Okumpura M, Isoda T. Conversion mechanism of perhydropolysilazane into silicon nitride-based ceramics. *J Mater Sci* 1994;**29**:4883–8.
21. Kern F, Gadow R. Liquid phase coating process for protective ceramic layers on carbon fibers. *Surf Coat Technol* 2002;**151–152**:418–23.
22. Ziegler G, Kleebe HJ, Motz G, Müller H, Traßl S, Weibelzahl W. Synthesis, microstructure and properties of SiCN ceramics prepared from tailored polymers. *Mater Chem Phys* 1999;**61**:55–63.
23. Bahloul D, Pereira M, Goursat P, Choong Kwet Yive NS, Corriu RJP. Preparation of silicon carbonitrides from an organosilicon polymer: I. Thermal decomposition of the cross-linked polysilazane. *J Am Ceram Soc* 1993;**76**(5):1156–62.
24. Bauer F, Decker U, Dierdorf A, Ernst H, Heller R, Liebe H, et al. Preparation of moisture curable polysilazane coatings: Part I. Elucidation of low temperature curing kinetics by FT-IR spectroscopy. *Prog Org Coat* 2005;**53**:183–90.
25. Kubo T, Tadaoka E, Kozuka H. Formation of silica coating films from spin-on polysilazane at room temperature and their stability in hot water. *J Mater Res* 2004;**19**:635–42.
26. Motz G, Hacker J, Ziegler G. Special modified silazanes for coatings, fibers and CMCs. *Ceram Eng Sci Proc* 2000;**21**:307–14.
27. Seyferth D, Wiseman GH. High-yield synthesis of Si_3N_4/SiC ceramic materials by pyrolysis of a novel polyorganosilazane. *J Am Ceram Soc* 1984;**67**(7):C132–3.
28. Oliver WC, Pharr GM. An improved technique for determining hardness and elastic modulus using load and displacement sensing indentation experiments. *J Mater Res* 1992;**7**:1564–83.
29. Nyquist RA, Putzig CL, Leugers MA, Kagel RO. *Handbook of infrared and Raman spectra of inorganic and organic salts, vol. 4: infrared spectra of inorganic compounds*. Academic press; 1997.
30. Lavedrine A, Bahloul D, Goursat P, Choong Kwet Yive NS, Corriu RJP, Leclerq D, et al. Pyrolysis of polyvinylsilazane precursors to silicon carbonitride. *J Eur Ceram Soc* 1991;**8**:221–7.
31. Cross TJ, Raj R, Prasad SV, Tallant DR. Synthesis and tribological behavior of silicon oxycarbonitride thin films derived from poly(urea)methyl vinyl silazane. *Int J Appl Ceram Technol* 2006;**3**:113–26.
32. Chavez R, Ionescu E, Balan C, Fasel C, Riedel R. Effect of ambient atmosphere on crosslinking of polysilazanes. *J Appl Polym Sci* 2011;**119**(2):794–802.
33. Choong Kwet Yive NS, Corriu RJP, Leclerq D, Mutin PH, Vioux A. Silicon carbonitride from polymeric precursors: thermal cross-linking and pyrolysis of oligosilazane model compounds. *Chem Mater* 1992;**4**:141–6.
34. Weibelzahl W. Herstellung und Eigenschaften von polymerabgeleiteten SiCN-Precursorkeramiken [Processing and properties of polymer-based SiCN-ceramics]. Dissertation University of Bayreuth; 2002.
35. Motz G, Ziegler G. Herstellung polymerer und keramischer Schichten über modifizierte. In: Ziegler G, Hermel W, Riedel H, editors. *Proc. Werkstoffwoche'98*. 1998. p. 667–71.
36. Colombo P, Paulson TE, Pantano CG. Synthesis of silicon carbide thin films with polycarbosilane (PCS). *J Am Ceram Soc* 1997;**80**:2333–40.

37. Colombo P, Paulson TE, Panano CG. Atmosphere effects in the processing of silicon carbide and silicon oxycarbide thin films and coatings. *J Sol–Gel Sci Technol* 1994;**2**:601–4.
38. Manufacturer's data. Heraeus Holding GmbH, Germany; 2011.
39. Cross TJ, Raj R, Prasad SV, Buchheit TE, Tallant DR. Mechanical and tribological behaviour of polymer-derived ceramics constituted from $SiC_xO_yN_z$. *J Am Ceram Soc* 2006;**89**(12):3706–14.
40. Galusek D, Riley FL, Riedel R. Nanoindentation of a polymer-derived amorphous silicon carbonitride ceramic. *J Am Ceram Soc* 2001;**84**(5):1164–6.
41. Allebrandt (Probst) D, Hoche H, Scheerer H, Broszeit E, Berger C. Oxidation resistance of SiAlCN: H-coatings. *Surf Coat Technol* 2007;**201**:5172–5.
42. Mucalo MR, Milestone NB, Vickridge IC, Swain MV. Preparation of ceramic coatings from pre-ceramic precursors. Part I: SiC and "Si_3N_4/Si_2N_2O" coatings on alumina substrates. *J Mater Sci* 1994;**29**:4487–99.